Interaction of Internal Ba^{2+} with a Cloned Ca^{2+}-dependent K^+ (h*slo*) Channel from Smooth Muscle

FELIPE DIAZ,* MARTIN WALLNER,‡ ENRICO STEFANI,‡ LIGIA TORO,‡ and RAMON LATORRE*

*Centro de Estudios Cientificos de Santiago, Casilla 16443, and Departamento de Biologia, Facultad de Ciencias, Universidad de Chile, Santiago Chile, and ‡Department of Anesthesiology, UCLA, Los Angeles, CA 90024

ABSTRACT We have studied potassium currents through a cloned Ca^{2+}-dependent K^+ channel (h*slo*) from human myometrium. Currents were recorded in inside-out macropatches from membranes of *Xenopus laevis* oocytes. In particular, the inactivation-like process that these channels show at high positive potentials was assessed in order to explore its molecular nature. This current inhibition conferred a bell shape to the current-voltage curves. The kinetic and voltage dependence of this process suggested the possibility of a Ba^{2+} block. There were the following similarities between the inactivation process observed at zero-added Ba^{2+} and the internal Ba^{2+} block of h*slo* channels: (*a*) in the steady state, the voltage dependence of the current inhibition observed at zero-added Ba^{2+} was the same as the voltage dependence of the Ba^{2+} block; (*b*) the time constant for recovery from current decay at zero-added Ba^{2+} was the same as the time constant for current recovery from Ba^{2+} blockade; and (*c*) current decay was largely suppressed in both cases by adding a Ba^{2+} chelator [(+)-18-crown-6-tetracarboxylic acid] to the internal solution. In our experimental conditions, we determined that the K_d for the complex chelator-Ba^{2+} is 1.6×10^{-10} M. We conclude that the current decay observed at zero-added Ba^{2+} to the internal solution is due to contaminant Ba^{2+} present in our solutions (~70 nM) and not to an intrinsic gating process. The Ba^{2+} blocking reaction in h*slo* channels is bimolecular. Ba^{2+} binds to a site ($K_d = 0.36 \pm 0.05$ mM at zero applied voltage) that senses 92 ± 25% of the potential drop from the internal membrane surface.

INTRODUCTION

Ca^{2+}-dependent K^+ (K_{Ca}) channels of large conductance originate sustained voltage-dependent currents (i.e., channels are noninactivating; Latorre et al., 1989). This rule has a notable exception in K_{Ca} channels of rat adrenal chromaffin cells (Solaro and Lingle, 1992). This channel shows a fast inactivation process that resembles that found in A-type potassium channels. Exposing to trypsin the cytoplasmic side of these channels removes fast inactivation. This last result suggests that the inactivating gate is a cytoplasmic portion of the channel-forming protein, probably the NH_2 terminal as found by Hoshi et al. (1991) for the case of *Shaker* K^+ channels.

We have recently cloned a K_{Ca} channel of large conductance from human myometrium (h*slo*; Wallner et al., 1995). As most voltage-dependent channels, h*slo* has six putative transmembrane segments, S1 to S6, a positively charged S4 segment, and a conserved region between S5 and S6, the pore region. In addition, this channel has four hydrophobic segments dubbed S7 to S10 not found in voltage-dependent channels (see also Butler et al., 1993 and Wei et al., 1994).

The h*slo* channel shares most of its properties with other K_{Ca} channels of large conductance. However, in inside-out patches and at large (≥ 100 mV) depolarizing voltages, current reaches a maximum and then decays with time (Walner et al., 1995; Tseng-Crank et al., 1994). Current inhibition confers a bell shape to the current-voltage curves. In the present work, we show that current inhibition at high voltages is not due to an intrinsic inactivation process. We found that addition to the internal solution of a crown ether, a member of the macrocyclic ligand family (e.g., Dietrich, 1985; Fig. 1), abolished current inactivation. The crown ether binds Ba^{2+} very tightly, much more than it binds Ca^{2+} (near two orders of magnitude difference). This chelator affects neither the Ca^{2+} activation nor the voltage-dependent characteristics of the channel. Therefore,

Address correspondence to Dr. Ligia Toro, Department of Anesthesiology, BH-612 Center for Health Sciences, UCLA School of Medicine, Box 951778, Los Angeles, CA 90095-1778.

J. GEN. PHYSIOL. © The Rockefeller University Press • 0022-1295/96/03/399/09 $2.00
Volume 107 March 1996 399–407

current decay is best explained by assuming that at large positive applied voltages, a time- and voltage-dependent blockade occurs induced by Ba^{2+} contamination of the internal solution. A detailed characterization of the internal Ba^{2+} blockade of this human K_{Ca} channel shows that the contaminant Ba^{2+} in our solutions is ~70 nM. The Ba^{2+} blocking rate is directly proportional to the internal free [Ba^{2+}]. Thus, the observed decrease in this rate with increasing crown ether concentration is a consequence of a free Ba^{2+} depletion of the internal solution. From the Ba^{2+} titration curve we obtained a value of 1.6×10^{-10} M for the dissociation constant of the chelator-Ba^{2+} complex. A preliminary report characterizing this kinetic process has appeared (Diaz et al., 1995).

MATERIALS AND METHODS

Oocyte Injection

The h*slo* cRNA, coding for a large conductance calcium-dependent potassium channel from human myometrium (Wallner et al., 1995; GenBank U11058), was synthesized as described previously. The synthesis was directed by the T7 promoter in the presence of capping nucleotide G(5')ppp(5')G. Collagenase treated *Xenopus laevis* oocytes (stage V-VI) were microinjected with 50 nl of 0.2-1 μg/μl mRNA in water. The oocytes were maintained at 18°C in an amphibian saline supplemented with gentamicin (50 μg/ml) and sodium pyruvate (2.5 mM).

Patch Recording

The vitelline membrane was manually removed and macroscopic currents were evoked in membrane patches in the inside-out configuration. Current records were obtained 4–7 d after the injection of the oocytes. The pipettes had 1 to 3 MΩ resistance and were filled with (millimolar): 110 potassium methanesulfonate (KMES), 10 Hepes, 2 $MgCl_2$, pH 7.0. The composition of the bath solution (intracellular membrane face) was (millimolar): 110 KMES, 10 HEPES, pH 7.0. This solution has 10 μM of contaminant Ca^{2+} or Ca^{2+} added at the indicated values. Free [Ca^{2+}] was measured with a Ca^{2+} electrode (World Precision Instruments, Sarasota, FL).

Membrane Preparation

Oocytes membranes were isolated according to Perez et al. (1994). Briefly, at day 10 after injection with h*slo* mRNA, 40–50 oocytes were rinsed and then homogenized in 300 mM sucrose in K^+ buffer (in millimolar): 600 KCl, 5 K-PIPES, pH 6.8 containing protease inhibitors. The homogenate was layered into a discontinuous 20:50% wt/vol sucrose gradient in K^+ buffer and centrifuged at 60,000 *g* for 30 min. The band at the 20:50% wt/vol sucrose interface was collected and diluted three times in the K^+ buffer. Membranes were centrifuged at 50,000 *g* for 45 min, and the pellet resuspended in 5 μl of solution A (in millimolar: 300 sucrose, 100 KCl, 5 K-MOPS, pH 6.8), divided in 1 μl portions and stored at −75°C.

Reconstitution into Bilayers

Membrane vesicles were fused with planar bilayers composed of phosphatidylethanolamine:phosphatidylserine:phosphatidylcholine in a ratio of 5:3:2 at 25 mg/ml in decane. The vesicles were applied with a glass rod to the preformed planar bilayer. Channel recordings were done in symmetrical 220 mM KCl, 10 mM HEPES, pH 7.0, and 50 μM added $CaCl_2$. The internal side of the channel was determined by the channel Ca^{2+} and voltage sensitivities.

Acquisition and Analysis

The current signal was digitized to a frequency equal to five times the filter cutoff frequency. The acquisition and basic analysis of the data were performed with pClamp 6.0 software (Axon Instruments, Inc., Foster City, CA) and custom made software. Burst time and blocked times were measured manually, considering as blocked times those periods longer than 500 ms.

Chemicals

A crown ether (a gift from Dr. Jacques Neyton), the (+)-18-Crown-6-tetracarboxylic acid (18C6TA) from E. Merck (Darmstadt, Germany) (also known as [+]-1,4,7,10,13,16-hexa-oxacyclooctadecane-2,3,11,12-tetracarboxylic acid; $C_{16}H_{24}O_{14}$, Fig. 1) was used to chelate the contaminant Ba^{2+} of the internal bath solution. The 18C6TA/cation stoichiometry is 1:1 (see Results). This crown ether also binds K^+ and Ca^{2+} with dissociation constants of 3.3×10^{-6} M and 10^{-8} M, respectively (Dietrich, 1985). Stock solutions were made in water.

RESULTS

Hslo Inside-Out Patch Currents Are Transient at High Voltages

We have previously shown that oocytes injected with cRNA transcribed from h*slo* express robust outward K^+ currents that are voltage dependent and Ca^{2+} sensitive (Wallner et al., 1995). Upon depolarization (up to 180 mV) and in the cell-attached mode, these currents increase to a certain level and remain constant for the whole duration of the depolarizing pulse (Fig. 2 *A*). In contrast, when inside-out patches are performed, large depolarizations induce a current that decays with time (Wallner et al., 1995; Tseng-Crank et al., 1994). As shown in Fig. 2 *B*, this current decay during the pulse is scarcely detectable at 80 mV, but as voltage is increased above this voltage value the rate of decay becomes faster and the steady state current becomes smaller (cf., current records obtained at 120 and 140 mV). Another

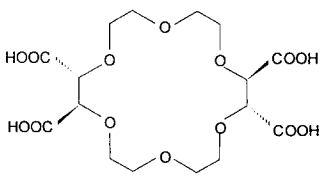

FIGURE 1. Chemical structure of the crown ether, (+)-18-Crown-6-tetracarboxylic acid (18C6TA), [(2R,3R,11R, 12R)-(+)-1,4,7,10,13, 16-hexa-oxacyclooctadecane-2,3,11, 12-tetracarboxylic acid].

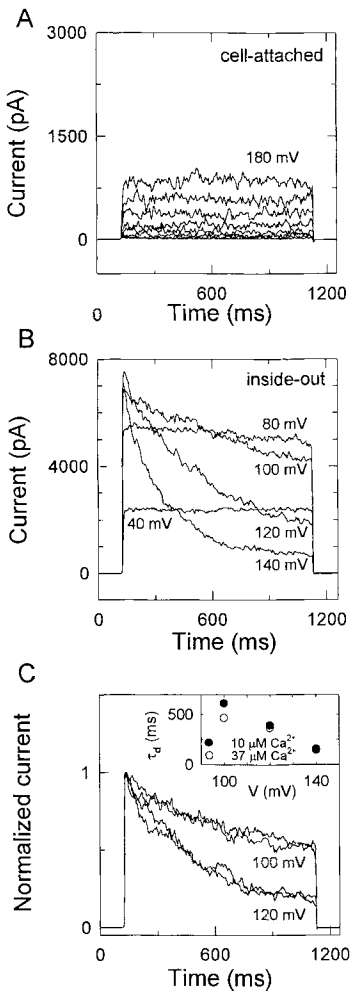

FIGURE 2. h*slo* macroscopic current shows a time- and voltage-dependent inhibition. Current traces in *A* (cell-attached) and *B* (inside-out) were recorded from the same patch. Solution was symmetrical 110 mM KMES and 10 μM Ca^{2+} (contaminant Ca^{2+}). For more details, see Methods. (*A*) The patch was held at 0 mV and stepped from 10 to 180 mV, for 1 s, every 10 mV. Traces correspond to 110 to 180 mV evoked currents. (*B*) Currents induced by voltage steps in the inside-out mode. Pulse duration of 1 s. Note the prominent current inhibition at 140 mV. (*C*) Superimposed trace currents at two $[Ca^{2+}]_i$ (10 μM and 37 μM) in an inside-out patch. Insert shows that current decay is practically indistinguishable at both $[Ca^{2+}]_i$.

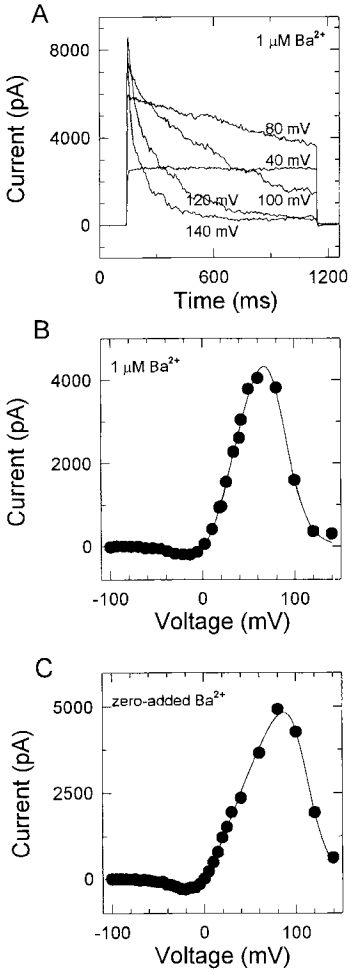

FIGURE 3. Internal Ba^{2+} induces an inhibition of h*slo* currents qualitatively similar to that seen with zero-added barium. (*A*) Current records obtained with 1 μM $BaCl_2$ added to the bath solution (intracellular membrane face). Voltage pulse values are shown next to each trace. Other conditions as in Fig. 1. (*B*) Steady-state *I–V* relationship constructed with the data shown in *A*. The current was measured at the end of each pulse. The records corresponding to the current values plotted for voltage values smaller than 40 mV are not shown. The fitting of Eq. 1 to the data (*continuous line*) gave the following parameters: G_{max} = 82 nS, z_{eq} = 1.7, V_0 = 11.0 mV, $K_d(0)$ = 1.37 mM and $z\delta$ = 2.15. (*C*) Steady state *I–V* relationship of data in Fig. 2 *B* in zero-added Ba^{2+}. The continuous line is the fit to the data using Eq. 1, and $z\delta$ (2.15) and $K_d(0)$ (1.37 mM) obtained from Fig. 3 *B* where 1 μM $[Ba^{2+}]$ is used. The fitted parameters were: G_{max} = 65 nS, z_{eq} = 2.01, V_0 = −5 mV, and "contaminant" [Ba] = 144 nM.

characteristic of the current decay, induced upon excision of the patch, is that it is not enhanced by increasing internal Ca^{2+} to 37 μM (Fig. 2 *C*). The inset in Fig. 2 *C* demonstrates that the time constant of decay is practically the same at both Ca^{2+} concentrations. It is apparent from Fig. 2 *B* (see also Fig. 3 *C*) that the current inhibition obtained at high voltages is a time- and voltage-dependent process. This process is reminiscent of the N-type inactivation present in some potassium channels (e.g., Hoshi et al., 1990; Solaro and Lingle, 1992). Nevertheless, at difference from N-type inactivation, the kinetic process reported here is too slow and develops at much higher voltages. On the other hand, the voltage dependence of current inhibition in the h*slo* channel is too high to be an inactivation process of the C-type found in some potassium channels. C-type inactivation is voltage independent over a range of −25

to 50 mV (Hoshi et al., 1991). The current decay is reminiscent of a voltage-dependent internal Ba^{2+} block (Armstrong and Taylor, 1980; Eaton and Brodwick, 1980). Therefore, we hypothesized that even though Ba^{2+} has not been added to the internal solution, this solution contains an effective contaminant Ba^{2+} concentration responsible for the current inhibition observed at high voltages.

Internal Barium Resembles the Inactivation Process Induced upon Excision of the Patch

We first analyzed the effect of 1 μM Ba^{2+} added to the internal solution (Fig. 3, *A* and *B*) and compared it with the inactivation induced in "zero-added" Ba^{2+} solution upon excision of the patch (Figs. 2 *B* and 3 *C*). Current records in 1 μM internal Ba^{2+} (Fig. 3 *A*) are qualitatively similar to those obtained in "zero-added" Ba^{2+} (Fig. 2 *B*), but there are some important quantitative differences. First, at any given voltage, the presence of 1 μM Ba^{2+} increases the rate of current decay; and second, inhibition is noticeable at lower voltages. The steady state current-voltage curves shown in Fig. 3, *B* and *C*, demonstrate that the depolarization needed to induce current decay is ~80 mV in 1 μM Ba^{2+} and ~100 mV in zero-added Ba^{2+}. In both cases, the data could be well fitted (*solid line*) to the equation:

$$I = \{G_{max}(V - E_K)/[1 + \exp(z_{eq}F(V - V_O)/RT)]\} [(1 + [Ba]/K_d(V))^{-1}], \quad (1)$$

where G_{max} is the maximum conductance; E_K is the K^+ equilibrium potential; z_{eq} is the equivalent number of gating charges; V_o is the voltage at which $G = 0.5G_{max}$; R, T, and F have their usual meaning; [Ba] is the barium concentration; and $K_d(V)$ is the dissociation constant for Ba^{2+} binding. Eq. 1 is the product of a Boltzmann distribution, describing the voltage activation of the channels times a Langmuir isotherm describing the fraction of current remaining after addition of Ba^{2+}. This equation assumes that inhibition by Ba^{2+} follows a single site titration curve (Vergara and Latorre, 1983; Perez et al., 1994), and that the dissociation constant for Ba^{2+} binding varies exponentially with voltage, as per Eq. 2 (Woodhull, 1973):

$$K_d(V) = K_d(0)\exp(-z\delta FV/RT), \quad (2)$$

where $K_d(0)$ is the dissociation constant at zero voltage, z is the valence of the blocking ion, and δ is the fraction of the total electrical potential drop across the membrane found at the Ba^{2+} binding site. The above assumptions are acceptable for other K_{Ca} channels (e.g., Vergara and Latorre, 1983), and in this paper we give evidence that they are reasonable for h*slo* as well (see next section).

The best fit to the data shown in Fig. 3 *B* (1 μM Ba^{2+}) using Eq. 1 was obtained with $z\delta = 2.15$ and a $K_d(0) = 1.37$ mM. Using these parameters, we then fitted the data in Fig. 3 *C* to obtain the putative [Ba^{2+}] concentration contaminating our internal solution. This fit gave a contaminant [Ba^{2+}] of 144 nM, a value in reasonable agreement with that calculated from kinetic parameters at different [Ba^{2+}] (see below and Fig. 5). The fit using Eq. 1 with the parameters obtained from the fit to the data of Fig. 3 *B* is remarkably good. We consider this result as the first evidence that current inhibition at zero-added Ba^{2+} is due to a blockade induced by a contaminant [Ba^{2+}].

Properties of Ba^{2+}-induced Blockade of hslo and Estimation of Contaminant [Ba^{2+}]

Fig. 4 shows that increasing [Ba^{2+}] speeds up the rate of current inhibition at constant voltage (*A*), and that recovery from blockade is independent of Ba^{2+} concentration (*B*). In addition, at constant [Ba^{2+}] current inhibition is well fitted to a single exponential function at all potentials tested (Fig. 3 *A*). These properties of Ba^{2+}-induced inhibition are in agreement with the single site model for Ba^{2+} block considered in Eq. 1, i.e.,

$$\text{open} \underset{\beta}{\overset{k_1[Ba]}{\rightleftarrows}} \text{blocked}.$$

SCHEME I

In this simple model, the fraction of blocked channels at equilibrium, f_{block}, the time constant of decay, τ_d, and the time constant for recovery, τ_r, are given by the relations:

$$f_{block} = k_1[Ba]/(k_1[Ba] + \beta) \quad (3)$$

$$\tau_d = 1/(k_1[Ba] + \beta) \quad (4)$$

$$\tau_r \approx 1/\beta. \quad (5)$$

The model predicts that the calculated rate of blocking, α, must be directly proportional to the internal free [Ba^{2+}] according to the relation:

$$\alpha = k_1[Ba]. \quad (6)$$

As illustrated in Fig. 5, one of the main predictions of a bimolecular blocking process is fulfilled. As demanded by Eq. 6, the ON blocking rate increases linearly with internal [Ba^{2+}] (Fig. 5 *A*). Notice, however, that the intercept at zero-added [Ba^{2+}] is not zero as predicted by Eq. 6 (Fig. 5 *A*, *inset*). We conclude that this non-zero value for α without added Ba^{2+} is due to the Ba^{2+} contaminating the internal solution. Extrapolation of the straight line drawn in Fig. 5 *A* to $\alpha = 0$ indicates that

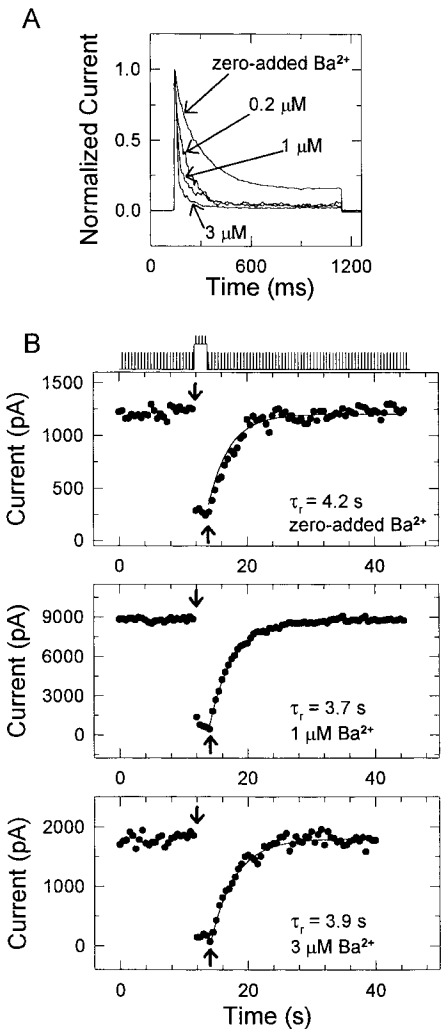

FIGURE 4. Internal Ba^{2+} speeds up the rate of current inhibition. (*A*) Currents induced by single voltage pulses to 150 mV from a holding voltage of zero mV, at zero-added $BaCl_2$ (*uppermost record*) and with the $BaCl_2$ concentrations showed next to each record. All the records were obtained with contaminant Ca^{2+} in the bath solution (10 μM). To compare blocking rates, currents were normalized to their maximum value. (*B*) Recovery times from Ba^{2+} blockade. An inside-out patch at a holding potential of 0 mV was pulsed continuously to 100 mV for 5 ms at 2 Hz. Arrows indicate the ON and the OFF of a 150 mV pulse stepped from the HP and lasting for two seconds. This pulse induced the blockade of hslo currents. Recovery of the current measured with the 100 mV test pulse follows an exponential time course (*solid line*). The current recovery is shown for three different patches. (*Top*) Zero-added $BaCl_2$; (*middle*) 1 μM $BaCl_2$; (*bottom*) 3 μM $BaCl_2$ added to the bath solution. Scheme on top of *B* corresponds to the pulse protocol.

this contamination amounts to 70 nM. These observations strongly support the idea that the contaminant Ba^{2+} is responsible for the current inhibition seen in the absence of added Ba^{2+}. Since in our experimental conditions Ba^{2+} is present during the recovery period,

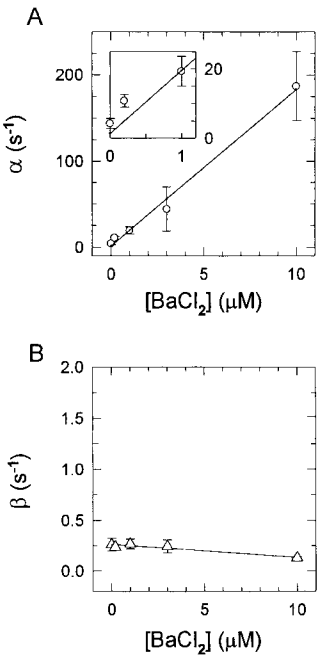

FIGURE 5. Ba^{2+} dependence of the ON and OFF blocking rates. (*A*) The ON rate of blockade, was calculated from currents evoked by voltage pulses to 150 mV, at the indicated internal $BaCl_2$ concentrations (see Fig. 4 *A*). The maximum and steady state current were measured and the relaxation of the current was fitted with a single exponential (τ_d). α was obtained using Eqs. 3 and 4 (see text). The straight line is the best fit to the experimental data. From the slope a $k_1 = 1.8 \times 10^7\ s^{-1}M^{-1}$ was obtained. Inset: Same plot is shown to note that with zero-added $BaCl_2$ the intercept is 1.4 s^{-1} and not zero as predicted by Eq. 6. (*B*) Time constant for recovery, $\tau_r = 1/\beta$, at 0 mV was obtained from experiments like those shown in Fig. 4 *B*. The internal $BaCl_2$ concentration was varied as indicated. The straight line is the best fit to the experimental points with a slope of $1.2 \times 10^4\ s^{-1}M^{-1}$ and an intercept of 0.26 s^{-1}. Bars represent the SE. *n* equals three to six experiments.

$\tau_r = 1/(k_1[Ba] + \beta)$. However, k_1 is voltage-dependent changing an e-fold/~27 mV (data not shown). This result implies that at 0 mV (the voltage at which the recovery from blockade is measured) $k_1[Ba]$ ranges from 0.0032 to 0.000022. This last value is 100- to 10,000-fold smaller than that of β. Thus, β is essentially independent of Ba^{2+} concentration in the [Ba] range tested (Fig. 5 *B*).

A Crown Ether that Forms Stable Complexes with Ba^{2+} in Solution Inhibits Current Decay in Zero-added Ba^{2+}

Fig. 6 *A* illustrates an example of current inhibition at 140 mV (zero-added Ba^{2+}). This inhibition is completely removed upon perfusion on the cytoplasmic side with a solution containing 50 μM of the Ba^{2+} chelator 18C6TA. Fig. 6 *B* shows the *I-V* relations for the same experiment in control conditions (zero-added Ba^{2+}) (*solid circles*) and after addition of 50 μM 18C6TA (*open circles*). Addition of the crown ether decreases the amount of current inhibition at all potentials tested. Fig. 6 *C* shows the normalized conductance obtained from the *I-V* relations shown in Fig. 6 *B*. Note that a discrete rightward shift of the normalized conductance vs voltage curve (~13 mV) occurs in the presence of the chelator. Since it is known that 18C6TA is able to bind Ca^{2+} (Dietrich, 1985), the shift in the *G-V* curve is most likely due to the chelation of Ca^{2+}. Measurements of

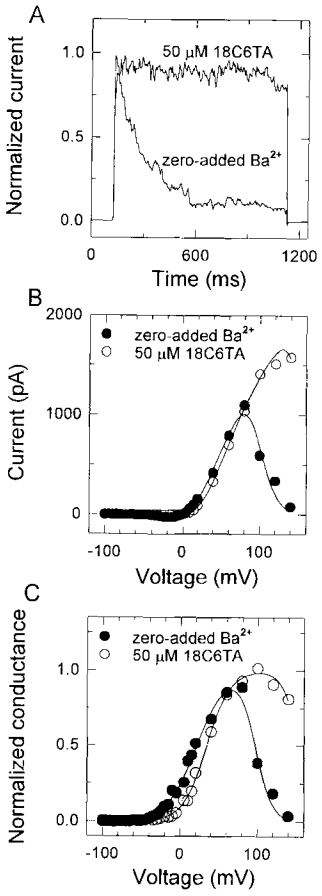

FIGURE 6. The Ba^{2+} chelator, 18C6TA, removes current inhibition. (*A*) Current traces in zero added Ba^{2+} and after perfusion of 50 μM 18C6TA in the same solution. Applied voltage was 140 mV from a holding potential of 0 mV. (*B*) *I–V* relations in control conditions (zero added Ba^{2+}, *filled circles*) and in the presence of 50 μM of 18C6TA in the internal bath solution of the experiment illustrated in *A*. (*C*). Corresponding conductance-voltage relationship. The continuous line is the fit to the data using the equation $G/G_{max} = I/[G_{max}(V - E_K)]$ where $I = \{G_{max}(V - E_K)/[1 + \exp(z_{eq}F(V - V_o)/RT)]\}$ $[(1 + [Ba]/K_{d(V)})^{-1}]$. Parameters are defined as in Eq. 1. Assuming a contaminant $[Ba^{2+}]$ of 70 nM (Fig. 5 *A*), fitted values for the zero-added Ba^{2+} curve were: G_{max} = 15 nS, z_{eq} = 1.35, V_0 = 22 mV, $K_d(0)$ = 646 μM and $z\delta$ = 2.4. The curve in presence of the Ba^{2+} chelator 18C6TA was fitted using $K_d(0)$ = 646 μM and $z\delta$ = 2.4. Fitted values were: G_{max} = 14 nS, z_{eq} = 1.7, V_0 = 35 mV and $[Ba^{2+}]$ after chelation = 0.27 nM. The shift in the *G-V* curve corresponds to a change in $[Ca^{2+}]$ from 10 to 7 μM, as measured with a Ca^{2+} electrode. In close agreement is the $[Ca^{2+}]$ value (8.7 μM) calculated using the K_d's of the chelator for Ba^{2+}, K^+ and Ca^{2+} (see text and Fig. 7).

free $[Ca^{2+}]$ with a Ca^{2+} electrode indicated that Ca^{2+} was diminished from 10 to 7 μM upon addition of 50 μM chelator. Using the Kd of the Ba^{2+}-chelator complex (see below), the K_d values for K^+ and Ca^{2+} complexes reported in the literature, and assuming that the contaminant Ba^{2+} is 70 nM (Fig. 5), we have calculated that 50 μM of 18C6TA diminishes Ca^{2+} from 10 to 8.7 μM and Ba^{2+} from 70 to 7 nM. Taken together, these experiments indicate that the decrease in the degree of current inhibition at high voltages by 18C6TA is most likely due to a removal of contaminant Ba^{2+} causing current blockade.

Removal of Ba^{2+}-induced Blockade by the Crown Ether

To further confirm the properties of the crown ether as a Ba^{2+} chelator we performed a dose-response curve in the presence of 1 μM Ba^{2+}. As expected for a relief of Ba^{2+} blockade by the crown ether, perfusion of increasing concentrations of [18C6TA] caused an increase in

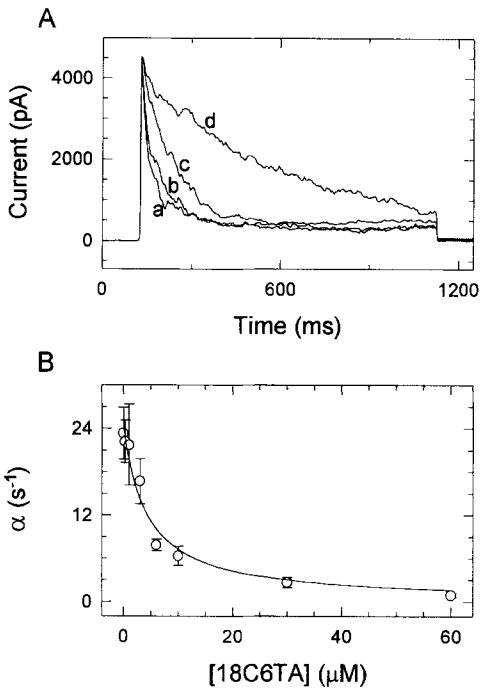

FIGURE 7. The Ba^{2+} chelator, 18C6TA, decreases the ON blocking rate. (*A*) Currents induced by voltage pulses to 150 mV with 1 μM internal $BaCl_2$ (trace *a*) or with the same $BaCl_2$ concentration plus 3 μM (trace *b*), 10 μM (trace *c*) or 30 μM (trace *d*) of 18C6TA. (*B*) On blocking rate (α) obtained with 1 μM internal $BaCl_2$ and the indicated concentrations of 18C6TA (*open circles*: experimental data ± SD from three to eight different experiments). The continuous line is the fit to the data using a Langmuir isotherm $\{\alpha = \alpha_{max}/(1+([18C6TA]/K)^N)$ with α_{max} = 22.9 s^{-1}, K = 4.54 mM, and N = 1.2.

the decay time constants (Fig. 7 *A*). Further analysis of the time course of the current inhibition shows that addition of the crown ether to the internal solution affects only the blocking rate constant for Ba^{2+} block. In Fig. 7 *B* we have plotted the rates of current decay at different crown ether concentrations. This curve can be fitted with a Langmuir isotherm with a Hill coefficient of near one (1.2). This finding is consistent with a complex 18C6TA-Ba having a 1:1 stoichiometry. We expect this result if the only effect of the chelator is to withdraw the Ba^{2+} present in the internal solution. Recalling Eq. 6, we interpreted Fig. 7 *B* as a Ba^{2+} titration curve. The free $[Ba^{2+}]$ at each [18C6TA] concentration ($[Ba]_{18C6TA}$) can be obtained by dividing α in the presence of 18C6TA (α_{18C6TA}) by α in its absence (α_o):

$$[Ba]_{18C6TA} = (\alpha_{18C6TA}/\alpha_o)\,[Ba^{2+}]_o, \qquad (7)$$

where $[Ba^{2+}]_o$ is the Ba^{2+} concentration in the absence of chelator (1 μM). Therefore, from Fig. 7 *B* we can calculate the unknown dissociation constant for the chelator-Ba^{2+} complex. The actual dissociation constant must be calculated considering the simultaneous

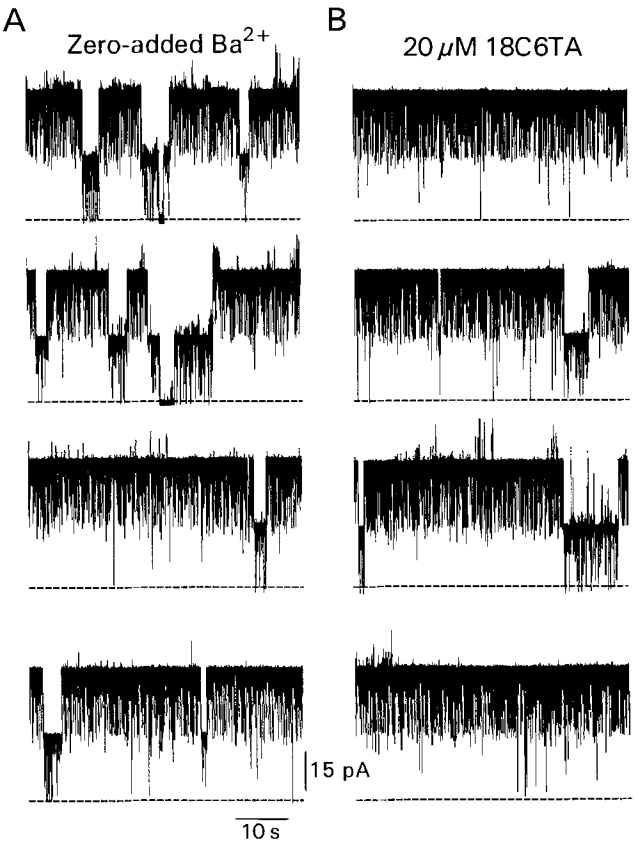

FIGURE 8. The Ba^{2+} chelator promotes changes in h*slo* single channel activity. hslo channels were incorporated into planar bilayers as described in Methods. (*A*) h*slo* channel records obtained in symmetrical 220 mM KCl, at +80 mV applied voltage. The intracellular Ca^{2+} concentration was 50 μM and zero-added Ba^{2+}. Long closed states can be explained as blocking periods (~4 s duration) by contaminant Ba^{2+}. (*B*) Same bilayer as in *A*, but after addition of 18C6TA to the internal side of the channels. [18C6TA] = 20 μM. Other experimental conditions are as in A.

equilibriums of 18C6TA with Ba^{2+}, Ca^{2+}, and K^+. Using dissociation constants for the 18C6TA-K^+ and 18C6TA-Ca^{2+} complexes of 3.3×10^{-6} and 10^{-8} M, respectively (Dietrich, 1985), we obtained a K_d for the 18C6TA-Ba^{2+} complex of 1.6×10^{-10} M. Crown ether compounds have cavities of different diameters in the center of the polyether rings. With a hole diameter of 2.6 to 3.2 Å (Pedersen, 1988), the 18-crown-6 family of crown ether compounds is particularly well suited to bind K^+ (2.66 Å) and Ba^{2+} (2.68 Å). Although the ratio K_d^K/K_d^{Ba} is ~ 56 for the 18-crown-6 compound (Dietrich, 1985), our results show that it increases to 2.06×10^4 for 18-crown-6-tetracarboxylic acid.

Relief of a Long Lived Closed State of Reconstituted hslo Channels by the Barium Chelator

Vergara and Latorre (1983) and Neyton and Miller (1988) observed in single-channel membranes the presence of long closing periods even at zero internal added Ba^{2+}. To inquire about the origin of these long closings, we reconstituted h*slo* channels into planar lipid bilayers. Fig. 8 *A* shows channel current records obtained at zero-added Ba^{2+}, at 80 mV. The records show that quiescent periods that can last for seconds interrupt channel activity. Fig. 8 *B* shows the same membrane after adding 20 μM 18C6TA to the cytoplasmic side of the channel. The chelator doubled the time the channel remains in the open state. Mean burst time was increased after perfusion of the crown ether, from 15 ± 3 s to 30 ± 8 s (no. events = 10 and 6, respectively). Furthermore, perfusion of the chelator did not modify the blocked times (3.9 ± 3 s, n = 9 events in control vs. 4 ± 3 s, n = 4 events after 18C6TA). These results give further evidence for the presence of contaminant Ba^{2+} in the internal solution producing long-lasting closed states, that explain current-inactivation at high depolarized potentials.

DISCUSSION

Contaminant Ba^{2+} Causes Current Inhibition at Large Voltages

In this work we show that at high positive applied voltages the current induced by the expression of h*slo* channel in *Xenopus laevis* oocytes decays with time. This decay is a consequence of a voltage-dependent binding of the Ba^{2+} contaminating our solutions to the channel and not to an intrinsic gating process. This contaminant Ba^{2+} amounts to ~70 nM. The $Ba^{2+}$and voltage dependence of the current decay is consistent with a simple model in which Ba^{2+} binds to a site within the membrane field. We can summarize the evidence supporting this conclusion as follows: (*a*) in steady state, the voltage dependence of current inhibition in zero-added Ba^{2+} is the same as the Ba^{2+} block voltage dependence; (*b*) the OFF rate of internal Ba^{2+} block is very similar to the rate for current recovery at zero-added Ba^{2+}; and (*c*) in the absence of added Ba^{2+}, current inhibition becomes negligible if a Ba^{2+} chelator is added to the internal side. The problem of K_{Ca} channel block by the contaminant amounts of Ba^{2+} present in the internal solution was first put forward by Neyton and Miller (1988). As found in the present work (Fig. 5), Neyton and Miller (1988) observed that the ON rate at zero-added Ba^{2+} is not zero. This rate decreased by 5–10-fold if sulfate replaced chloride in the internal solution. Since the solubility product of $BaSO_4$ is 1.05×10^{-10}, in the presence of sulfate the internal [Ba^{2+}] is kept < 1 nM. Furthermore, the ON rates obtained at zero-added Ba^{2+} in the present work and by Neyton and Miller (1988) are similar (~5 s^{-1}).

Vergara and Latorre (1983) interpreted the long closings present in their single K_{Ca} channel records as

intervals of time the channel was blocked by Ca^{2+}. In the present study, we show that 18C6TA increases the mean h*slo* channel burst time but does not modify the mean time of the long closings observed at zero-added Ba^{2+}. Since this crown ether specifically chelates Ba^{2+}, the contaminant Ba^{2+} present in the internal solution very likely promotes the long closed periods. There is great similarity between the mean block time of the single channel and the time constant for macroscopic current recovery at zero-added Ba^{2+}. This result strongly suggests that the nature of the macroscopic current inhibition resides in the long closing events observed at the single-channel level.

Ba^{2+} Block in hslo Channels

Ba^{2+} block of the h*slo* channel shows most of the characteristics of the Ba^{2+} block of other K_{Ca} channels of large unitary conductance (Vergara and Latorre, 1983; Hunter et al., 1984; Benham et al., 1985; Gitter et al., 1987; Guggino et al., 1987; Pérez et al., 1994). The dissociation constant of the Ba^{2+} channel complex is in the micromolar range. The block is voltage dependent, as though Ba^{2+} bound to a site at 92 ± 25% of the way through the voltage drop from the inside. This observation provides strong support to the idea that the site of Ba^{2+} blockade is located within the conduction pore of the h*slo* channel. Most of the voltage dependence of the blocking reaction resides in the association rate constant (data not shown). The fact that the association rate is voltage dependent, whereas the dissociation is not, suggests that the peak of the energy barrier that Ba^{2+} needs to jump is quite near the binding site (Vergara and Latorre, 1983).

Nature of the Binding of Ba^{2+} to K^+ Channels

Vergara and Latorre (1983) hypothesized that the strong blocking effect of Ba^{2+} on Ca^{2+}-activated K^+ channels of large conductance is due to the similarity in the radius of Ba^{2+} and K^+ (see also Armstrong and Taylor, 1980 and Eaton and Brodwick, 1980). The divalent nature of Ba^{2+} made a very stable Ba-channel complex. In fact, the overall dissociation rate from the channel for K^+ is $\sim 10^8$ s^{-1} (Latorre and Miller, 1983; Moczydlowski et al., 1985) which is 4×10^8-fold faster than the Ba^{2+} dissociation rate measured in the present work (~ 0.25 s^{-1}). K_{Ca} channels allow conduction of only alkali monovalent cations of similar size (e.g., K^+ and Rb^+) suggesting the existence of a narrow region defined as a selectivity filter (Hille, 1975, Latorre and Miller, 1983). Therefore, it is possible that Ba^{2+} binds tightly to this structure (Miller et al., 1987). The degree of identity between the pore (*P*) regions of K_{Ca} channels and *Shaker* K^+ channels is very high (Heginbotham et al., 1994; Latorre, 1994). In the latter channels, extensive mutagenesis experiments suggest that (Heginbotham et al., 1994): first, ion discrimination takes place in this region; and second, the atoms that interact with K^+ could be carbonyl atoms from the protein backbone. Second, in K_{Ca} and in *Shaker* K^+ channels an aspartate residue follows the highly conserved sequence gly-tyr-gly. The side chain of this negatively charged amino acid projects into the pore lumen in *Shaker* K^+ channels (Lü and Miller, 1995). Kirsch et al. (1995) showed that when aspartate 378 is mutated to threonine in $K_V2.1$ channels, the selectivity sequence for alkali cations is unaltered, but the P_{Na}/P_K ratio increases fivefold. The gly-tyr-gly triad is crucial in determining *Shaker* K^+ channel cation selectivity (Heginbotham et al., 1992, 1994). The sequence gly-tyr-gly may play the role of a selectivity filter. On the other hand, the ring of carboxyl groups of the aspartate residues present in K^+ channels may provide the Coulombic interactions that stabilize the Ba^{2+}-channel complex.

We wish to thank Dr. Jacques Neyton who introduced us to the crown ether compound used in the present work and for communicating his results before publication. We would also like to thank Dr O. Alvarez and A. Oberhauser for comments on the manuscript.

This work was supported by NIH grants HL54970 (to L. Toro) and GM50550 (to E. Stefani); Chilean grants FNI 2950028 (to F. Diaz) and FNI-1940227 (to R. Latorre); and Human Frontier in Sciences Program, European Communities Research Contract, SAREC (Sweden) and a group of Chilean private companies (COPEC, CMPC, CGEI, ENERSIS, CAP, IBM, La Escondida, and Xerox Chile) (to R. Latorre).

Original version received 23 October 1995 and accepted version received 6 December 1995.

REFERENCES

Armstrong, C.M., and S.R. Taylor. 1980. Interaction of barium ions with potassium channels in squid giant axons. *Biophys. J.* 30:473–488.

Benham, C.D., T.B. Bolton, K.J. Lang, and T. Takewaki. 1985. The mechanisms of action of Ba^{2+} and TEA on single Ca^{2+}-activated K^+ channels in arterial and intestinal smooth muscle cell mem-

brane. *Pflügers Archiv. Eur. J. Physiol.* 403:120–127.

Butler, A., S. Tsunoda, D.P. McCobb, A. Wei, and L. Salkoff. 1993. m*Slo*, a complex mouse gene encoding "maxi" calcium-activated potassium channels. *Science (Wash. DC).* 261:221–224.

Diaz, F., M. Wallner, E. Stefani, L. Toro, and R. Latorre. 1995. Barium blockade of a cloned Ca^{2+}-activated K^+ channel (*hslo*) expressed in *Xenopus laevis* oocytes. *Biophys. J.* 68:A29. (Abstr.)

Dietrich, B. 1985. Coordination chemistry of alkali and alkaline-earth cations with macrocyclic ligands. *J. Chem. Educ.* 62:954–964.

Eaton, D.C., and M.S. Brodwick. 1980. Effects of barium on the potassium conductance of squid axon. *J. Gen. Physiol.* 75:727–750.

Gitter, A.H., K.W. Beyenbach, C.W. Chadwick, P. Gross, W. Minuth, and E. Fromter. 1987. High conductance K^+ channels in apical membranes of principal cells cultured from rabbit renal cortical collecting duct anlagen. *Pflügers Archiv. Eur. J. Physiol.* 408:282–290.

Guggino, S.E., W.B. Guggino, N. Gree, and B. Sacktor. 1987. Blocking agents of Ca^{2+}-activated K^+ channels in cultured medullary thick ascending limb cells. *Am. J. Physiol.* 252:C128–C137.

Heginbotham, L., T. Abramson, and R. MacKinnon. 1992. A functional connection between pores of distantly related ion channels as revealed by mutant K^+ channels. *Science (Wash. DC).* 258: 1152–1155.

Heginbotham, L., Z. Lu, T. Abramson, and R. MacKinnon. 1994. Mutations in the K^+ channel signature sequence. *Biophys. J.* 66: 1061–1067.

Hoshi, T., W.N. Zagotta, and R.W. Aldrich. 1990. Biophysical and molecular mechanisms of Shaker potassium channel inactivation. *Science (Wash. DC).* 250:533–538.

Hoshi, T., W.N. Zagotta, and R. Aldrich. 1991. Two types of inactivation in *Shaker* K^+ channels: effects of alterations in the carboxy-terminal region. *Neuron.* 7:547–556.

Hunter, M., A.G. Lopes, E. Boulpape, and G.H. Giebish. 1984. Single channel recording of single Ca^{2+}-activated K^+ channels in the apical membrane of cortical collecting tubules. *Proc. Natl. Acad. Sci. USA.* 81:4237–4239.

Kirsch, G.E., J.M. Pascual, and C-C. Shieh. 1995. Functional role of a conserved aspartate in the external mouth of voltage-dependent potassium channels. *Biophys. J.* 68:1804–1813.

Latorre, R. 1994. Molecular workings of large conductance (maxi) Ca^{2+}-activated K^+ channels. *In* Membrane Channels: Molecular and Cellular Physiology. C. Peracchia, editor. Academic Press, NY. 79–102.

Latorre, R., and C. Miller. 1983. Conduction and selectivity in potassium channels. *J. Membr. Biol.* 71:11–30.

Latorre, R., A. Oberhauser, P. Labarca, and A. Alvarez. 1989. Varieties of calcium-activated potassium channels. *Ann. Rev. Physiol.* 51:385–399.

Lu, Q., and C. Miller. 1995. Silver as a probe of pore-forming residues in a potassium channel. *Science (Wash. DC).* 268:304–307.

Miller, C., R. Latorre, and I. Reisin. 1987. Coupling of voltage-dependent gating and Ba^{2+} block in the high conductance Ca^{2+}-activated K^+ channel. *J. Gen. Physiol.* 90:427–449.

Moczydlowski, E., O. Alvarez, C. Vergara, and R. Latorre. 1985. Effect of phospholipid surface charge on the conductance and gating of a Ca^{2+}-activated K^+ channel in planar lipid bilayers. *J. Membr. Biol.* 83:273–282.

Neyton, J., and C. Miller. 1988. Potassium blocks barium permeation through a Ca^{2+}-activated K^+ channel. *J. Gen. Physiol.* 92: 549–567.

Pérez, G., A. Lagrutta, J.P. Adelman, and L. Toro. 1994. Reconstitution of expressed K_{Ca} channels from *Xenopus* oocytes into lipid bilayers. *Biophys. J.* 66:1022–1027.

Solaro, C.R., and C.J. Lingle. 1992. Trypsin-sensitive, rapid inactivation of a calcium-activated potassium channel. *Science (Wash. DC).* 257:1694–1698.

Vergara, C., and R. Latorre. 1983. Kinetics of Ca^{2+}-activated K^+ channels from rabbit muscle incorporated into planar bilayers. Evidence of a Ca^{2+} and Ba^{2+} blockade. *J. Gen. Physiol.* 82:543–568.

Tseng-Crank, J., C.D. Foster, J.D. Krause, R. Mertz, N. Godinot, T. J. DiChiara, and P.H. Reinhart. 1994. Cloning, expression, and distribution of functionally distinct Ca^{2+}-activated K^+ channel isoforms from human brain. *Neuron.* 13:1315–1330.

Wallner, M., P. Meera, M. Ottolia, G. Kaczorowski, R. Latorre, M. Garcia, E. Stefani, and L. Toro. 1995. Cloning, expression and modulation by a β subunit of a maxi K_{Ca} channel from human myometrium. *Recept. Channels.* 3:185–199.

Wei, A., C. Solaro, C. Lingle, and L. Salkoff. 1994. Calcium sensitivity of BK-type K_{Ca} channels determined by a separable domain. *Neuron.* 13:671–681.

Woodhull, A.M. 1973. Ionic blockage of sodium channels in nerve. *J. Gen. Physiol.* 61:687–708.